Impact of the Green Light Program on haze in the North China Plain, China

Xin Long[1,3,7], Xuexi Tie[1,2,3,4,5*], Jiamao Zhou[3], Wenting Dai[3], Xueke Li[6], Tian Feng[1], Guohui Li[1,3], Junji Cao[1,3], and Zhisheng An[1]

[1]State Key Laboratory of Loess and Quaternary Geology, SKLLQG, Institute of Earth Environment, Chinese Academy of Sciences, Xi'an 710061, China

[2]Center for Excellence in Urban Atmospheric Environment, Institute of Urban Environment, Chinese Academy of Sciences, Xiamen 361021, China

[3]Key Laboratory of Aerosol Chemistry and Physics, Institute of Earth Environment, Chinese Academy of Sciences, Xi'an 710061, China

[4]Shanghai Key Laboratory of Meteorology and Health, Shanghai, 200030, China

[5]National Center for Atmospheric Research, Boulder, CO 80303, USA

[6]Department of Geography, University of Connecticut, Storrs, Mansfield, CT 06269, USA

[7]School of Environment Science and Engineering, Southern University of Science and Technology, Shenzhen 518055, China

Correspondence to: Xuexi Tie (email: xxtie@ucar.edu)

Abstract. As the world's largest developing country, China undergoes the ever-increasing demand for electricity during the past few decades. In 1996, China launched the Green Lights Program (GLP), which became a national energy conservation activity for saving lighting electricity, as well as an effective reduction of the coal consumption for power generation. Despite of the great success of the GLP, its effects on haze have not been investigated and well understood. This study focused to assess the potential coal-saving induced by the improvement of luminous efficacy, the core of the GLP, and to estimate the consequent effects on the haze in the North China Plain (NCP), where located a large amount of power plants and often engulfed by severe haze. The estimated potential coal-saving induced by the GLP can reach a massive value of 120–323 million tons, accounting for 6.7–18.0% of the total coal consumption for thermal power generation in China. There was a massive potential emission reductions of air pollutants from thermal power generation in the NCP, which was estimated to be 20.0–53.8 Gg for NOx and 6.9–18.7 Gg for SO_2 in December 2015. The potential emission reductions induced by the GLP plays important roles in the haze formation, because the NOx and SO_2 are important precursors for the formation of particles. To assess the impact of the GLP on haze, sensitive studies were conducted by applying a regional chemical/dynamical model (WRF-CHEM). The model results suggest that in the case of lower limit emission reduction, the $PM_{2.5}$ concentration decreased by 2–5 μg m^{-3} in large areas of the NCP. In the case of upper limit emission reduction, there was much more remarkable decrease in $PM_{2.5}$ concentration (4–10 μg m^{-3}). This study is a good example to illustrate that scientific innovation can induce important benefits on environment issues, such as haze.

Keywords: Green Light Programs; thermal power plants; Haze in NCP; WRF-CHEM

1 Introduction

As the world's largest developing country, China undergoes the ever-increasing demand for electricity during the past few decades. Artificial lighting is an important part of China's energy consumption, accounting for a quite stable share of about 10–14% of the total electricity consumption (Lv and Lv, 2012; Zheng et al., 2016). Also, the lighting demand in China is predicted to increase continuously, with a projected average annual growth rate of 4.3% from 2002 to 2020 (Liu, 2009). With principal objective of alleviating shortage of electricity, China has launched the Green Lights Program (GLP) in 1996, with the core of aiming at replacing low-efficiency lighting lamps by high-efficiency ones. Since then, the GLP has become a national energy conservation activity for saving lighting electricity (Lin, 1999), and has been highlighted continuously in the nation's 9^{th}–12^{th} Five-Year Plan (1996–2015) (Guo et al., 2017).

With the object of providing high-quality efficient lighting products, the GLP is undoubtedly a useful electricity saving measure. Nonetheless, driven by the accelerated economic increase, the thermal power electricity has experienced an ever-increasing trend in the past decades, as well as the associated coal consumption for thermal power generation. Thermal power generation is the primary electricity source in China, contributing to about 72–78% of the total electricity (NBS, 2000–2016). In 2015, the coal consumption for thermal power generation in China raised to a massive value of about 1.8 billion tons, which was 3.2 times of that in 2000. And the coal consumption for thermal power generation in China was 2.7 times of that in the USA, which was reported to be 670 million tons (https://www.eia.gov/totalenergy/data/browser/, last accessed on 20 December, 2018).

Due to the significant use of coal, thermal power generation is one of the dominant emission contributors to anthropogenic air pollutants in China (Tie and Cao, 2010; Wang and Hao, 2012; Wang et al., 2015b). The power sector contributes significantly to air pollutants of the nitrogen oxides (NOx), the sulfur dioxide (SO_2), and the particulate mater (PM) (Zhao et al., 2013; Huang et al., 2016). The pollutants of SO_2 and NOx are the precursors of secondary pollutants of ozone (O_3), and secondary aerosols (Seinfeld et al., 1998; Laurent et al., 2014). It is also reported that emission from power sector is a major contributor to particulate sulfate, and nitrate (Zhang et al., 2012). The emissions from thermal power generation in China can also transport to a long distance, causing regional/global air pollutions (Tie et al., 2001; Huang et al., 2016). Considering the important contributions to air pollutants, controlling emissions from thermal power generation is a vital strategy for the improvement of air quality in China.

Distinguished from the ever-increasing trend of thermal power electricity and the associated coal consumption, the increase trends of SO_2 and NOx emissions from thermal power generation are curbed and even change to decrease (Liu et al., 2015). This is caused by the nation-wide project of utilizing emission control facilities during 2005 to 2015, such as installing flue-gas desulfurization/denitrification systems and optimizing the generation fleet mix (Liu et al., 2015; Huang et al., 2016). Influenced by the technological changes that have occurred in the power sector, the air pollutant emissions from power generation have been significantly reduced. Emission reductions of air pollutants can substantially reduce the aerosol loading, and thus influenced the boundary layer, which is inherently connected to air pollution (Li et al., 2017). The interactions between aerosol and boundary layer can influence the surface ozone significantly, and more attention should be paid when controlling ozone pollution (Gao et al., 2018). However, the thermal power generation is still identified to be with massive air pollutant emissions, involving 5.1 million tons of NOx, 4.0 million tons of SO_2, and 0.8 millions tons of PM in 2015 (Tong et al., 2018). Under high standards of ultra-low emission power units, the staggering total amount of coal consumption becomes a vital challenge for emission control from thermal power generation.

With ambitious and comprehensive efforts, the success of the GLP resulted in about 59 billion kWh of accumulated electricity savings from 1996 to 2005 (SCIO, 2006), and about 14.4 billion kWh of annual electricity savings from 2006 to 2010 (Lv and Lv, 2012). It is reported that the GLP has produced climate benefit for environment, reducing 17 million tons of CO_2 and 530 thousand tons of SO_2 emissions from 1996 to 2005 (Guo and Pachauri, 2017). Aside from emission reductions, the GLP is benefit to coal-saving from the thermal power generation, which inherently connected to air quality in China (Liu et al., 2015; Huang et al., 2016; Hu et al., 2016).

However, few studies have been so far dedicated to estimate the effectiveness of the GLP in controlling air pollution on a regional scale. In the North China Plain (NCP), the thermal power plants are distributed very densely, resulting in massive emissions of air pollutants (Liu et al., 2015). As a result, the GLP could produce significant energy-saving and reduce the associated air pollutant emissions from thermal power generation. Although the GLP is under the strong and sustained government commitment, however, there is no built-in mechanism for monitoring the GLP and without regularly issued official program assessment reports (Guo and Pachauri, 2017). During the past decades, the Chinese government has published only one report regarding the performance of the GLP (NDRC, 2005). There are several articles and books for summarizing the GLP from time to time by the Energy Research Institute under Chinas' National Development and Reform Commission, providing information for an assessment of the GLP (Yu and Zhou, 2001; Liu, 2006; Liu and Zhao, 2011; Liu, 2012; Lv and Lv, 2012; Gao and Zheng, 2016). Previous studies do not well investigate the effects of the GLP on air pollution, such as the resultant emission reductions of air pollutants, or the consequent effects on haze.

We quantified the effect of the GLP on the haze in the NCP, a severe air polluted region in China. The study included satellite measurements and numerical model studies (WRF-CHEM). We first investigated the lighting coal consumption and resultant coal-saving induced by the GLP utilizing the satellite nighttime lights (NTL) data (Elvidge et al., 2009), which has been widely used to estimate the consumption of energy and electricity (He et al., 2013; Huang et al., 2014). Then we evaluated the potential emission reductions and resultant effects on air pollution in the NCP using the WRF-CHEM model. This study provided an overall perspective on gaps of the unevaluated potential benefits to haze induced by the GLP, which can inspire more macroscopic and interdisciplinary analysis in long-term national activities based on NTL datasets. We summarized the data, the methodology, and the WRF-CHEM model description in Section 2. Results and discussions were presented in Section 3, followed by the summaries and conclusions in Section 4.

2 Data and methodology

2.1 The NTL and emissions form power sector

In order to understand the spatial distributions of lighting electricity consumption, we investigated the version 4 of the Defense Meteorological Satellite Program Operational Line Scanner (DMSP/OLS) NTL time series data from 1992 to 2013 (Elvidge et al., 2014). The dataset available at: https://ngdc.noaa.gov/eog/dmsp/downloadV4composites.html. We selected the stable light datasets, which are the cloud-free composites using all the archived DMSP/OLS smooth resolution data for calendar years. The images represent the average intensity of NTL with DN values ranging from 0 to 63 in 30 arc-second grids-cells (about 1 km spatial resolution). The 1992 and the 2013 datasets were used to investigate the different status of NTL before and after the GLP. Considering the differences between the sensors, differences in the crossing times of the satellites, and degradation of the sensors (Elvidge et al., 2009; Elvidge et al., 2014), we inter-calibrated the NTL datasets followed a second order regression model (Elvidge et al., 2014). **Figure 1** shows the spatial distributions of the DMSP/OLS NTL data. We found that the nighttime lights were increased significantly from 1992 to 2013, both in lighting intensity and spatial coverage, especially in the regions of eastern China, including the NCP, the Pearl River Delta, and the Yangtze River Delta. The rapid increase in the nighttime lights implicates that the lighting electricity were greatly increased.

Based on the statistics of National Bureau of Statistics of China (NBS, 2000–2016) and previous studies (Liu et al., 2015; Tong et al., 2018), Figure 2 summarized the annual thermal power electricity, the total coal consumption for thermal power generation, and the air pollutant emissions (SO_2, NO_x and $PM_{2.5}$) from thermal power plants in China. The ever-increasing demand of electricity, increased from 2000 (about 10^{12} kW h) to 2015 (about 4×10^{12} kW h), was most likely driven by the rapid increase of economics. The SO_2 emission from power sector increased before 2005, corresponding to the increase of coal consumption. While after 2006, the SO_2 emission from power sector started to decrease sharply, and this is mainly caused by the widespread emission control strategies of installation of flue gas desulfurization systems and the substitution of lower sulfur fuel (Liu et al., 2016). Distinguished from the increase trend of NO_x emission from transportation (Hu et al., 2016), the decrease of NO_x emission from power sector started to decrease in 2012 due to the significant technological improvement of coal-consumption weighted mean NOx removal efficiency (Hu et al., 2016; Tong et al., 2018). Compared to the gas-phase emissions of SO_2 and NOx, the direct emission of particles ($PM_{2.5}$) was relatively small (Liu et al., 2015; Tong et al., 2018). The large portion of gas-phase emissions and small portion of $PM_{2.5}$ emissions (Fig. 2) from thermal power generation indicated that the most $PM_{2.5}$ emitted from the power plants might be in the phase of secondary particles.

The GLP focused on improving the luminous efficacy, saving lighting electricity, and thus reducing the coal consumption and air pollutant emissions from thermal power generation, which is inherently connected to air quality. As the business as usual condition (i.e., without the GLP), the increased lighting demand could cause more significant increase in thermal power electricity, and produce stronger demand of coal consumption for power generation during the past decades. This study was to assess the potential effects induced by the GLP on haze in the NCP, and also to display a good example to illustrate that scientific innovation can induce important benefits on environment issues. To assess the impacts of the GLP on the severe air polluted region in China, such as in the NCP, several important tools and data were used in this study, including a regional chemical/dynamical model (WRF-CHEM), satellite data (DMSP/OLS and S-NPP), and surface measurements of air pollutants.

2.2 Description of the WRF-CHEM model

We used a specific version of the WRF-CHEM model (Grell et al., 2005). The model included a new flexible gas-phase chemical module and the Models3 community multi-scale air quality (CMAQ) aerosol module developed by the US EPA (Binkowski and Roselle, 2003). The model included the dry deposition (Wesely 1989) and wet deposition followed the CMAQ method. The impacts of aerosols and clouds on the photochemistry (Li et al., 2011b) were considered by the photolysis rates calculation in the fast radiation transfer model (Tie et al., 2003; Li et al., 2005). The inorganic aerosols (Nenes et al., 1998) were predicted using the ISORROPIA Version 1.7. We also used a non-traditional secondary organic aerosol (SOA) model, including the volatility basis-set modeling approach and SOA contributions from glyoxal and methylglyoxal. Detailed information about the WRF-CHEM model can be found in previous studies (Li et al., 2010; Li et al., 2011a; Li et al., 2011b; Li et al., 2012).

In the present study, we simulated severe haze from 1 to 31 December 2015 in the NCP. The domain, centered at the point of (116° E, 38° N), was composed horizontally of 300 by 300 grid points spaced with a resolution of 6 km (**Fig. 3**) and vertically with 35 sigma levels. The physical parameterizations included the microphysics scheme (Hong and Lim 2006), the Mellor–Yamada–Janjic turbulent kinetic energy planetary boundary layer scheme (Janjić, 2002), the unified Noah land-surface model (Chen and Dudhia, 2001), the Goddard long wave radiation parameterization(Chou and Suarez, 1999), and the shortwave radiation parameterization (Chou et al., 2001). Meteorological initial and boundary conditions were obtained from the 1° by 1° reanalysis data of National Centers for Environmental Prediction (Kalnay et al., 1996). The spin-up time of WRF-CHEM model is 3 days. The chemical initial and boundary conditions were constrained from the 6 h output of Model of Ozone and Related chemical Tracers, Version 4 (Horowitz et al., 2003).

We utilized the anthropogenic emission inventory developed by Tsinghua University (Zhang et al., 2009), including anthropogenic emission sources from transportation, agriculture, industry and power generation and residential. The dataset can be accessible from the website of MEIC (http://www.meicmodel.org), providing for the community a publically accessible emission dataset over China with regular updates. The emission inventory used in the present study was updated and improved for the year 2015. In addition, the emissions of SO_2, NOx, and CO have been adjusted according to the observations during the period. Emissions from biogenic sources were calculated online using the Model of Emissions of Gases and Aerosol from Nature model (MEGAN) (Guenther et al. 2006).

2.3 Analysis of satellite data and model domain

Since the launch of the Suomi-National Polar-orbiting Partnership satellite in 2011, the Day/Night Band for the Visible Infrared Imaging Radiometer Suite (VIIRS DNB) has been widely used in recent studies, which confirmed to establish empirical relationships with energy use (Román and Stokes, 2015; Coscieme et al., 2014). To some extent, the VIIRS NTL dataset (in 15 arc-second grids-cells, about 500 m) are superior to the DMSP/OLS NTL dataset (Elvidge et al., 2013). In the present study, we used the version 1 of VIIRS NTL dataset to investigate the consumption of lighting electricity in each province, defined as provincial dynamics as follow.

$$PD_i = \frac{\sum_i L_j \times S_j}{\sum_w L_j \times S_j} \quad (1)$$

where i denotes the provincial domain, and w is the nationwide domain. j is the pixel of VIIRS NTL dataset. S is the area of pixel j. L is the NTL radiance. The annual VIIRS NTL dataset contains cloud-free average of NTL radiance by excluding any data impacted by stray light, and further screening out the fires and other ephemeral lights and background (non-lights). The dataset is available at: https://ngdc.noaa.gov/eog/viirs/download_dnb_composites.html.

The distribution of VIIRS NTL radiance in 2015 (**Fig. S1**) was similar as the DMSP/OLS DN values (**Fig. 1)**. The high values of annual NTL radiance were concentrated in the densely populated and industrial developed areas of China (**Fig. S1a**), such as the NCP, the Yangtze

River Delta, and the Pearl River Delta. There were “hot spot” located in some megacities, such as the Beijing, Tianjin, Shanghai, Guangzhou, where the NTL radiance can reach as high as 20 $mW/m^2/sr$. Statistically, 12.8% of these China's land areas consumes 58.3% of lighting electricity consumption. The high values of provincial dynamics also concentrated on these regions, and all the provincial dynamics exceeding 5% were coastal cities (**Fig. S1b**). In the NCP, in addition to the high usage of lighting, there is a large amount of power plants (Liu et al., 2015). We selected the NCP (**Fig. 3**) as the region of interest. In addition, there are extensive measurement sites of pollutants in the domain (the green crosses in **Fig. 3**).

2.4 Estimation of coal-saving induced by the GLP

According to the analysis for the Chinese GLP program (Guo and Pachauri, 2017), the lighting activities can be defined as three clusters according to their usages: **(C_1)** For outdoor lighting, such as road lights; **(C_2)** household usage, mainly for residential applications; **(C_3)** commercial and industrial buildings. In practice, the core of the GLP is to improve luminous efficiency, replacing low-efficiency lighting lamps by high-efficiency ones. The details of the GLP program were as follows. For **C_1**, the High Pressure Sodium lamps (HPS) and Metal Halide (MH) lamps are primarily used to replace High Pressure Mercury-vapor lamps (HPM). For **C_2**, the Compact Fluorescent Lamps (CFLs) are used to replace incandescent lamps (ILs). For **C_3**, the T8/T5 fluorescent tubes are used to replace T12/T10 fluorescent tubes. The emerging LED lamps were not covered, however, it promotes to each of the above cluster (Pan, 2018; Wang, 2017; Asolkar and Dr., 2017; Xie et al., 2016; Ge et al., 2016; Edirisinghe et al., 2016). Here the LED lamps were allocated proportionally based on the proportions of the lighting electricity consumption of **C_1**, **C_2**, and **C_3**.

According to the classification above, we estimated the current equivalent luminous efficacy

(ELE_{GLP}) weighted by the proportion of their lighting electricity consumption. To investigate the potential effectiveness of the GLP, we also calculated the equivalent luminous efficacy without the implementation of the GLP (ELE_{no-GLP}).

$$ELE_{GLP} = \sum f_k LE_{k,GLP} \quad (2)$$

$$ELE_{no-GLP} = \sum f_k LE_{k,no-GLP} \quad (3)$$

where k denotes the specified cluster of lighting lamps. f_k is the proportion of lighting electricity consumed by the k^{th} cluster lamps; $LE_{k,GLP}$ and $LE_{k,no-GLP}$ denote the equivalent luminous efficacy of the k^{th} cluster lamps with and without the improvement of lighting efficacy induced by the GLP. The ELE is a comprehensive parameter to reflect the lighting efficacy. In terms of current consumption levels of lighting electricity, the lighting coal consumption for power generation is proportional to ELE. As a result, the potential coal-saving induced by the GLP (dC) can be estimated by:

$$dC = C_0 \times \frac{ELE_{no-GLP} - ELE_{GLP}}{ELE_{GLP}} \quad (4)$$

where C_0 denotes the current coal consumption for thermal power generation. To get the spatial distribution of potential provincial coal-savings (dC_i), we spatially scaled the total potential coal-saving (dC) according to the provincial dynamics factor (PD_i), which is calculated based on the spatiotemporal dynamic of electric power consumption in each province (Elvidge et al., 1997; Chen and Nordhaus, 2011; He et al., 2013).

$$dC_i = dC \times PD_i \quad (5)$$

where i denotes the province; PD_i reflects provincial dynamics of lighting coal consumption, which was explained in **Eq. 1**.

Here we focus on the potential emission reductions derived from the potential lighting electricity savings induced by the GLP. And the emission reduction was confined at the improvement of luminous efficacy, which is the core of the GLP (Guo et al., 2017). Between the base case (with the GLP) and sensitivity cases (without the GLP), the coal-saving induced by the GLP was estimated with the same purification efficiency of air pollutant emissions between the base case (with the GLP) and sensitivity cases (without the GLP). And the ratio of power electricity goes to lights is same with the ratio of artificial lighting to the total electricity consumption, which is 10–14% (Lv and Lv, 2012; Zheng et al., 2016).

It is worth noting that, there were uncertainties in the present study. Thermal power generation is the primary electricity source in China, contributing to about 72–78% of the total electricity (NBS, 2000–2016), which indicates at least 6% uncertainty in the estimation. Lv and Lv (2012) and Zheng et al. (2016) estimate the ratio of artificial lighting to the total electricity consumption, and the ratio is 10–14%, which indicates about 4% uncertainty in the estimation.

Based on the current anthropogenic emission inventory from MEIC (Multi-resolution emission inventory for China) (Liu et al., 2015; Zhang et al., 2009), the potential emission reduction ($dE_{power,spec}$) induced by the GLP was proportional to the associated potential coal-saving for the thermal power generation.

$$\frac{dE_{power,spec}}{dC} = \frac{E_{power,spec}}{C_0} \qquad (6)$$

where $E_{power,spec}$ denotes the emission inventory from the thermal power sector; *spec* is the specify air pollutant of WRF-CHEM species. dC and C_0 are the same as that in Eq. 4.

2.5 WRF-CHEM sensitive studies

Based on previous studies (Guo and Pachauri, 2017), the effective luminous efficacy (ELE) increased from 50 lm/W to 70–140 lm/W for $\mathbf{C_1}$, from 15 lm/W to 50–60 lm/W for $\mathbf{C_2}$, and from 70–80 lm/W to 80–105 lm/W for $\mathbf{C_3}$. Simultaneously, the LED has experienced a fast growth since 2011, with the market share of LED lamps reached 32% in 2015, and the high efficacy LED lamps with 150 lm/W had been industrialized production in China (Gao and Zheng, 2016). Here we treated the market share of LED lamps as the proportion of its lighting electricity consumption. The regional diversity of LED market share would significantly influence the emission reductions derived by the luminous efficacy improvement induced by the GLP. However, the lighting electricity is transported from the power plants. The spatial dynamics of emission reductions induced by the GLP should be consistent with the distribution of power plants and the related coal consumption. The effects from regional diversity of LED market share was finally included in the distribution of emissions from power sector. The LED market share was allocated proportionally to the clusters according to the research of Zheng et al., (2016), which reported the proportion of its lighting electricity consumption with $\mathbf{C_1}$**:** $\mathbf{C_2}$**:** $\mathbf{C_3}$ being 31.6%: 19.7%: 48.7%. More detailed information can be founded in **Table 1**.

The estimated ELE values have uncertainties for both low and high efficient lamps, ranging from 52.8 to 57.7 lm/W and from 96.2 to 120.9 lm/W for the ELE with or without the GLP, respectively (see **Table 1**). In addition, the estimate of lighting electricity accounts for 10–14% of the total electricity (Zheng et al., 2016; Lv and Lv, 2012). As a result, the model sensitive studies included low-limit and high-limit of electricity power savings. To account for all of the uncertain ranges, in the lower limit model simulation, the thermal power was estimated to increase 6.7%, without the GLP. In the higher limit model simulation, the thermal power was estimated to increase 18.7%, without the GLP. **Figure 4** shows that under lower and higher limit assumptions, the potential coal-savings induced by the GLP were 120–323 million tons, respectively. According to these estimates into the reference emission inventory ($E_{0,spec}$), the emission of pollutants, with the 3 cases (reference, low-limit, and high-limit) were estimated and shown in **Table 2**. The reference emission inventory is developed by Tsinghua University

(Zhang et al., 2009), including current emission levels of thermal power plants (with considering GLP).

Table 2 shows the emissions from power generation, including the NOx, SO_2, PM2.5 and other species (represented with X), such as the BC, PM coarse, VOC, and so on. The direct emission of $PM_{2.5}$ was much smaller than the direct emission of SO_2 and NOx in gas-phase. The $PM_{2.5}$ concentrations included two different parts from thermal power plants. One was from the direct emission of $PM_{2.5}$ in particle phase, and the other was the secondary particle ($PM_{2.5}$), which was formed from the chemical transformation from SO_2 and NOx. As a result, the large effect of the GLP on haze was due to the changes in the emissions of SO_2 and NOx from the thermal power plants.

3 Results and discussions

3.1 Model evaluation

To better understand the effect of the GLP on the haze in the NCP, we first conducted an evaluation of the WRF-CHEM model performance. The modeled results were compared to the hourly near-surface concentrations of CO, SO_2, NO_2, and $PM_{2.5}$. The data was measured by the Ministry of Ecology and Environmental of China, and are accessible from the website http://www.aqistudy.cn/. The locations of the measurement sites show in **Fig. 3**.

The model results were evaluated by calculating the following statistical parameters, including normalized mean bias (*NMB*), the index of agreement (*IOA*), and the correlation coefficient (*r*). These parameters were used to assess the performance of REF case in simulations against measurements.

$$NMB = \frac{\sum_{i=1}^{N}(P_i - O_i)}{\sum_{i=1}^{N} O_i} \qquad (7)$$

$$IOA = 1 - \frac{\sum_{i=1}^{N}(P_i - O_i)^2}{\sum_{i=1}^{N}(|P_i - \bar{O}| + |O_i - \bar{O}|)^2} \quad (8)$$

$$r = \frac{\sum_{i=1}^{N}(P_i - \bar{P})(O_i - \bar{O})}{[\sum_{i=1}^{N}(P_i - \bar{P})^2 \sum_{i=1}^{N}(O_i - \bar{O})^2]^{\frac{1}{2}}} \quad (9)$$

where P_i and O_i are the calculated and observed air pollutant concentrations respectively. *N* is the total number of the predictions used for comparisons. $\bar{P}$ and $\bar{O}$ represent the average predictions and observations, respectively. The *IOA* ranges from 0 to 1, with 1 showing perfect agreement of the prediction with the observation. The *r* ranges from -1 to 1, with 1 implicating perfect spatial consistency of observation and prediction.

Figure 5 shows the temporal variation of modeled results with the measured values during December 2015. The measured values of pollutants ($PM_{2.5}$, NO_2, SO_2, and CO) averaged in the NCP were compared with the modeled results. The results indicate that there were strong episodes of the hourly $PM_{2.5}$ mass concentrations, with the highest values of exceeding 300 μg m^{-3}, implicating that several haze events occurred during the period. There are several peak values of $PM_{2.5}$ concentrations occurred during period, with a highest peak occurred between 22-24th December. Comparing with CO temporal variability, the temporal variations between CO and $PM_{2.5}$ were similar. The modeled $PM_{2.5}$ and CO captured the strong temporal variation, with the *IOA* of 0.98 and the *NMB* of 1.3% for $PM_{2.5}$ mass concentrations and *IOA* of 0.89 and the *NMB* of 4.3% for CO mass concentrations. Since the CO variability was mainly determined by meteorological conditions, the similarity of the temporal variability suggested that the meteorological conditions had important contribution to the several peak values of the episode, and the model simulation well captured the meteorological conditions during the study period.

Although there was a similarity of the temporal variability between $PM_{2.5}$ and CO, the magnitude of the variability of CO was smaller than variability of $PM_{2.5}$, suggesting that in addition to the meteorological conditions, the chemical formation also played important roles for producing the high peaks of $PM_{2.5}$ concentrations. It is important to simulate the measured temporal variations of SO_2 and NOx, because they are important chemical precursors (Seinfeld and Pandis, 1998; Laurent. et al., 2014), and are the major pollutants emitted from the thermal power plants (**Table 2**). As shown in **Fig. 5**, both the measured and modeled SO_2 and NOx had several episodes, which were corresponding to the episodes of the $PM_{2.5}$. The parameters between the measured and modeled results were acceptable, with the *IOA* of 0.83 and the *NMB* of 1.3% for SO_2, and *IOA* of 0.93 and the *NMB* of 6.1% for NOx. It is interesting to note that the occurrences of the peak of SO_2 and NOx are about 1-2 days ahead of the peak of $PM_{2.5}$. One of the explanations was that there was chemical conversion from gas-phase of SO_2 and NOx to particle phase of $PM_{2.5}$, resulting in the time lag between the peaks of SO_2-NOx and $PM_{2.5}$, because SO_2 and NOx were the precursors of $PM_{2.5}$ (Seinfeld and Pandis, 1998; Laurent. et al., 2014). As we state in the previous sections, the large effect of the GLP on haze was due to the changes in the emissions of SO_2 and NOx from the thermal power plants. The good statistical performance of the modeled SO_2 and NOx provided confident to use the model to study the GLP effects on haze in the NCP region.

In order to do more thoughtful validation of the model performance, **Figure 6** shows the measured and modeled spatial distributions of $PM_{2.5}$, SO_2, and NOx in the NCP. The model generally reproduced the spatial variations of $PM_{2.5}$, NO_2, and SO_2, capturing the spatial characters. For example, the SO_2 were largely emitted from thermal power plants and steel industrials, which were large point sources. As a result, both the modeled and measured SO_2 appeared as scattered distributions (see **Fig. 6d**). The correlation coefficients (r) between the measured and modeled results were 0.86, 0.68, and 0.70 for $PM_{2.5}$, NO_2, and SO_2, respectively.

In general, the NCP encountered severe haze events during the December 2015. The statistical analysis showed that the WRF-CHEM model reasonably captured the spatial and temporal variations of haze in the NCP, although some model biases existed. The model validation provided a confident to the further model studies.

3.2 Potential benefit of the GLP to haze in the NCP

There are massive emissions of NOx and SO_2 from thermal power plants in the research domain, producing 299.1 Gg and 103.7 Gg (**Tab. 1**) during the December 2015, for NOx and SO_2, respectively. There is more emission amount of NOx than SO_2, because the SO_2 emissions from power had been significantly declined since 2005, whereas the NOx emissions were slightly declined (see **Fig. 2**) due to lower effective NOx emission control facilities (Liu et al., 2015; Huang et al., 2016).

According to the estimate of 6.7–18.0% of potential coal-saving induced by the GLP (**Sect. 2.5**), the potential emission reductions from power generation were calculated base on **Eq. 6**, and the emission reductions of NOx and SO_2 induced by the GLP were estimated for the WRF-CHEM model sensitive studies. **Figure 7** shows the spatial distributions of changes in NOx and SO_2 emissions in the research domain, especially the provinces of Hebei, Henan, and Shandong within the NCP, where concentrated most of the power plants (Liu et al., 2015). The results show that under low limit estimate, without the GLP, the NOx and SO_2 emissions would be increased by 20.0 Gg and 6.9 Gg, respectively, in December 2015. Under high limit estimate, without the GLP, the NOx and SO_2 emissions would be increased by 53.8 Gg and 18.7 Gg in the NCP. These large emission changes without the GLP could cause important effects on the aerosol pollution. In the following sections, the GLP effect on the reduction of aerosol pollution was investigated by using the WRF-CHEM model.

According to the lower and upper limits of emission reductions induced by the GLP, we evaluated their resultant effects on air pollutants ($PM_{2.5}$, NO_2, and SO_2), which are estimated by the difference of the SEN-GLP cases and the REF case (**Fig. 8**). The result shows that the GLP has important effects on $PM_{2.5}$ concentrations (see **Figs 8a and 8b**), implicating the remarkable benefit to haze in the NCP. In the case of lower limit emission reduction, the $PM_{2.5}$ concentrations could be decreased by 2–5 μg m^{-3} in large areas within the NCP, such as the southeastern Hebei, northeastern Henan, and western Shandong (**Fig. 8a**). In the case of upper limit emission reduction, there is much more remarkable decrease in $PM_{2.5}$ concentrations (4–10 μg m^{-3}) in wider areas within the NCP (**Fig. 8b**). We can also find large-scale reductions of NO_2 and SO_2 in the NCP (**Fig. 8c-f**). For example, in high limit case, the reduction of NO_2 ranges from 1–8 μg m^{-3}, and the reduction of SO_2 ranges from 1–4 μg m^{-3}. We also display the species variations ($PM_{2.5}$, NO_2, and SO_2) within the areas (see red-square in Fig. 8) with high $PM_{2.5}$ changes induced by the GLP (**Fig. S2**).

Although the influence of the GLP is to decrease $PM_{2.5}$ concentrations, there were some slight increases in $PM_{2.5}$ concentrations in north of NCP. As indicated in **Table 2**, the directly emission of $PM_{2.5}$ was less than the gas-phase emissions of NOx and SO_2, which suggested that the decrease of $PM_{2.5}$ by applying the GLP was mainly due to the chemical conversions from gas-phase NOx and SO_2 to nitrate and sulfate particles (Seinfeld et al., 1998; Laurent et al., 2014). The slight increase of the $PM_{2.5}$ concentrations may be induced by the changes in O_3 concentrations, because the chemical conversion from NOx and SO_2 to nitrate and sulfate requires the atmospheric oxidants like O_3. As shown in **Fig. S3**, there is slight increase of O_3 (1–2 μg m^{-3}) due to the GLP, and the slightly increase the oxidation of SO_2, which may cause some enhancement of sulfate concentrations (Wang et al., 2015a; Xue et al., 2016). Apparently, the NO_2 reductions are more remarkable because of the more noteworthy NOx emission reductions induced by the GLP.

The GLP resulted in significant reduction of potential pollutant emissions from the thermal power generation, corresponding to potential benefit in alleviating haze in the NCP, although with few fluctuated deteriorations. It also benefits the pollution of NOx and SO_2 in the NCP.

4 Summary

For replacing low-efficiency lighting lamps by high-efficiency ones, the Green Lights Program (GLP) is a national energy conservation activity for saving lighting electricity consumption in China, resulting in an effective reduction of coal consumption for power generation. However, despite of the great success of the GLP in lighting electricity, the effects of the GLP on haze are not investigated and well understood. In the present study, we try to assess the potential coal-saving induced by the GLP, and to estimate its resultant benefit to the haze in the NCP, China, where often suffer from severe haze. First, we used the satellite dataset of nighttime lights to evaluate the associated saving of lighting electricity consumption and its resultant coal-saving in the NCP. Second, we estimated the emission reductions from thermal power generation induced by the GLP, based on the emission inventory developed by Tsinghua University (Zhang et al., 2009). Finally, we applied the WRF-CHEM model to evaluate the potential effects of the GLP on the haze in the NCP. The model results had been evaluated by a comparison with surface measurements. And two sensitivity experiments were conducted to explore the role of the GLP in benefiting the haze. Some important results are summarized as follows.

1. Due to the rapid increase in the economics, the demand of electricity is largely enhanced in China. As a result, the thermal power electricity increase from 2000 (about 10^{12} kW h) to

2015 (about 4×10^{12} kW h), suggesting that the lighting electricity consumption could produce higher emissions of air pollutants in the densely populated and industrial developed regions of China.

2. The GLP program significantly improves in lighting efficiency by 66.8–128.8%, implicating 6.7–18.0% of potential savings for electricity consumption, as well as potential coal-savings in thermal power generation.
3. The estimated potential coal-saving induced by the GLP can reach a massive value of 120–323 million tons, accounting for 6.7–18.0% of the total coal consumption for thermal power generation in China. As a result, there is a massive potential emission reduction of air pollutants from thermal power generation, involving 20.0–53.8 Gg for NOx and 6.9–18.7 Gg for SO_2 in the NCP of China. The reductions of these emissions play important roles in reducing the haze formation in the NCP, because NOx and SO_2 are important precursors for the particles.
4. The reduction of NOx and SO_2 from power plants produces a remarkable benefit to haze in the NCP. The sensitive studies by using the WRF-CHEM model shows that the GLP has important effects on $PM_{2.5}$ concentrations in the NCP. In the lower limit case, the $PM_{2.5}$ concentrations could be decreased by 2–5 μg m^{-3} in large areas within the NCP. In the upper limit case, there is much more remarkable decrease in $PM_{2.5}$ concentrations (4–10 μg m^{-3}) in wider areas within the NCP.

This study is a good example to illustrate that scientific innovation can induce important benefits on environment issues, such as haze.

Data availability

The real-time O3 and PM2.5 observations are accessible for the public on the website http://106.37.208.233:20035/. One can also access the historic pro- file of observed ambient pollutants through visiting http://www.aqistudy.cn/

The DMSP/OLS) NTL time series data are accessible for the public on the website https://ngdc.noaa.gov/eog/dmsp/downloadV4composites.html

The VIIRS NTL dataset are accessible for the public on the website https://ngdc.noaa.gov/eog/viirs/download_dnb_composites.html

Author contributions

X. T., and X. L. designed the study. X.-K. L. provided measurement data. J.-M.Z., W.-T. D., F. T., G.-H. L. analyzed the data. X. L. and X. T. wrote the manuscript. J. C. and Z. A. overviewed the paper. All authors commented on the manuscript.

Competing interests

The authors declare that they have no conflict of interest.

Acknowledgement

This work is supported by the National Natural Science Foundation of China (NSFC) under Grant No. 41430424 and 41730108, and the Ministry of Science and Technology of China under Grant No. 2016YFC0203400. The National Center for Atmospheric Research is sponsored by the National Science Foundation.

Reference

Asolkar, K., and Dr., A. S. S.: Energy Efficient Intelligent Household LED Lighting System Based On Daylight Illumination, Int. J. Eng. Tech., 9, 4258-4264, 2017.

Binkowski, F. S., and Roselle, S. J.: Models - 3 Community Multiscale Air Quality (CMAQ) model aerosol component 1. Model description, J. Geophys. Res., 108, 2003.

Chen, F., and Dudhia, J.: Coupling an advanced land surface–hydrology model with the Penn State–NCAR MM5 modeling system. Part II: Preliminary model validation, Mon. Weather Rev., 129, 587-604, 2001.

Chen, X., and Nordhaus, W. D.: Using luminosity data as a proxy for economic statistics, P. Nat. Acad. Sci. USA, 108, 8589-8594, 2011.

Chou, M. D., and Suarez, M. J.: A solar radiation parameterization for atmospheric studies, NASA TM-104606, Nasa Tech.memo, 15, 1999.

Chou, M. D., Suarez, M. J., Liang, X. Z., Yan, M. H., and Cote, C.: A Thermal Infrared Radiation Parameterization for Atmos. Stud., Max J, 2001.

Coscieme, L., Pulselli, F. M., Bastianoni, S., Elvidge, C. D., Anderson, S., and Sutton, P. C.: A Thermodynamic Geography: Night-Time Satellite Imagery as a Proxy Measure of Emergy, Ambio, 43, 969-979, 2014.

Edirisinghe, K., Abeyweera, R., and Senanayake, N. S.: Evaluation of Effectiveness of LED Lighting in Buildings, 2016.

Elvidge, C. D., Baugh, K. E., Kihn, E. A., Kroehl, H. W., Davis, E. R., and Davis, C. W.: Relation between satellite observed visible-near infrared emissions, population, economic activity and electric power consumption, Int. J. Remote Sens., 18, 1373-1379, 1997.

Elvidge, C. D., Sutton, P. C., Ghosh, T., Tuttle, B. T., Baugh, K. E., Bhaduri, B., and Bright, E.: A global poverty map derived from satellite data, Comput. Geosci., 35, 1652-1660, 2009.

Elvidge, C. D., Baugh, K. E., Zhizhin, M., and Hsu, F. C.: Why VIIRS data are superior to DMSP for mapping nighttime lights, P. Asia-Pac. Adv. Netw., 35, 62-69, 2013.

Elvidge, C. D., Hsu, K. E., Baugh, K., and Ghosh, T.: National Trends in Satellite Observed Lighting: 1992-2012, Global Urban Monitoring and Assessment Through Earth Observation, Boca Raton, FL, USA, 2014,

Gao, F., and Zheng, B.: Review of Development and Implementation of the Green Lighting Project in China, China Illum. Eng. J., 2016.

Gao, J., Zhu, B., Xiao, H., Kang, H., Pan, C., Wang, D., & Wang, H. 2018. Effects of black carbon and boundary layer interaction on surface ozone in Nanjing, China. Atmospheric Chemistry and Physics, 18(10), 7081-7094.

Ge, A., Shu, H., Chen, D., Cai, J., Chen, J., and Zhu, L.: Optical design of a road lighting luminaire using a chip-on-board LED array, Lighting Res. Technol., 49, 2016.

Grell, G. A., Peckham, S. E., Schmitz, R., McKeen, S. A., Frost, G., Skamarock, W. C., and Eder, B.: Fully coupled "online" chemistry within the WRF model, Atmos. Environ., 39, 6957-6975, 2005.

Guenther, A., Karl, T., Harley, P., Wiedinmeyer, C., Palmer, P. I., and Geron, C.: Estimates of global terrestrial isoprene emission using MEGAN, Atmos. Chem. Phys., 6, 3181-3210, 2006.

Guo, F., and Pachauri, S.: China's Green Lights Program: A review and assessment, Energ. Policy, 110, 31-39, 2017.

He, C., Ma, Q., Liu, Z., and Zhang, Q.: Modeling the spatiotemporal dynamics of electric power consumption in Mainland China using saturation-corrected DMSP/OLS nighttime stable light data, Int. J. Digit. Earth, 10.1080/17538947.2013.822026, 2013.

Hong, S.-Y., and Lim, J.-O. J.: The WRF Single-Moment 6-Class Microphysics Scheme (WSM6), Asia-Pac. J. Atmos. Sci., 42, 129-151, 2006.

Horowitz, L. W., Walters, S., Mauzerall, D. L., Emmons, L. K., Rasch, P. J., Granier, C., Tie, X., Lamarque, J. F., Schultz, M. G., and Tyndall, G. S.: A global simulation of tropospheric ozone and related tracers: Description and evaluation of MOZART, version 2, J. Geophys. Res. Atmos., 108, ACH 16-11, 2003.

Hu, J., Huang, L., Chen, M., He, G., and Zhang, H.: Impacts of power generation on air quality in China—Part II: Future scenarios, Resour. Conserv. Recy., 121, 115–127, 2016.

Huang, L., Hu, J., Chen, M., and Zhang, H.: Impacts of power generation on air quality in China—part I: An overview, Resour. Conserv. Recy., 2016.

Huang, Q., Yang, X., Gao, B., Yang, Y., and Zhao, Y.: Application of DMSP/OLS Nighttime Light Images: A Meta-Analysis and a Systematic Literature Review, Remote Sens., 6, 6844-6866, 2014.

Janjić, Z. I.: Nonsingular implementation of the Mellor–Yamada level 2.5 scheme in the NCEP Meso model, NCEP office note, 437, 61, 2002.

Kalnay, E., Kanamitsu, M., Kistler, R., Collins, W., Deaven, D., Gandin, L., Iredell, M., Saha, S., White, G., and Woollen, J.: The NCEP/NCAR 40-Year Reanalysis Project, Bull.amer.meteor Soc, 77, 437-472, 1996.

Laurent, O., Hu, J., Li, L., Cockburn, M., Escobedo, L., Kleeman, M. J., and Wu, J.: Sources and contents of air pollution affecting term low birth weight in Los Angeles County, California, 2001-2008, Environ. Res., 134, 488-495, 2014.

Li, G., Zhang, R., Fan, J., and Tie, X.: Impacts of black carbon aerosol on photolysis and ozone, J. Geophys. Res., 110, 2005.

Li, G., Lei, W., Zavala, M., Volkamer, R., Dusanter, S., Stevens, P., and Molina, L.: Impacts of HONO sources on the photochemistry in Mexico City during the MCMA-2006/MILAGO Campaign, Atmos. Chem. Phys., 10, 6551-6567, 2010.

Li, G., Bei, N., Tie, X., and Molina, L.: Aerosol effects on the photochemistry in Mexico City during MCMA-2006/MILAGRO campaign, Atmos. Chem. Phys., 11, 5169-5182, 2011a.

Li, G., Zavala, M., Lei, W., Tsimpidi, A., Karydis, V., Pandis, S. N., Canagaratna, M., and Molina, L.: Simulations of organic aerosol concentrations in Mexico City using the WRF-CHEM model during the MCMA-2006/MILAGRO campaign, Atmos. Chem. Phys., 11, 3789-3809, 2011b.

Li, G., Lei, W., Bei, N., and Molina, L.: Contribution of garbage burning to chloride and PM 2.5 in Mexico City, Atmos. Chem. Phys., 12, 8751-8761, 2012.

Li, Z., Guo, J., Ding, A., Liao, H., Liu, J., Sun, Y., ... & Zhu, B., 2017. Aerosol and boundary-layer interactions and impact on air quality. National Science Review, 4(6), 810-833.

Lin, J.: China green lights program: A review and recommendations, Lawrence Berkeley National Laboratory, 1999.

Liu, F., Zhang, Q., Tong, D., Zheng, B., Li, M., Huo, H., and He, K. B.: High-resolution inventory of technologies, activities, and emissions of coal-fired power plants in China from

1990 to 2010, Atmos. Chem. Phys., 15, 18787-18837, 2015.

Liu, H.: China's Green Lights Program: review of the past ten years and prospect, Energ. China, 28, 17-20, 2006.

Liu, H.: The concept and practice of green lights, China Electric Power Press, 2009.

Liu, H., and Zhao, J. P.: The Implementation Manual of China Green Lights, China Environ. Sci. Press, Beijing, 2011.

Liu, H.: China's Green Lights Program in the past 20 years, J. China Illum. Eng., 23, 12-17, 2012.

Long, X., Bei, N., Wu, J., Li, X., Feng, T., Xing, L., Zhao, S., Cao, J., Tie, X., An, Z., and Li, G.: Does afforestation deteriorate haze pollution in Beijing–Tianjin–Hebei (BTH), China?, Atmos. Chem. Phys., 18, 10869-10879, 10.5194/acp-18-10869-2018, 2018.

Lv, F., and Lv, W. B.: The Progress and Prospect of Green Lights Program in China, China Illum. Eng. J., 23, 1-6, 2012.

NBS, National Bureau of Statistics, China Statistical Yearbook 2000-2016, China Statistics Press, Beijing, available at: http://www.stats.gov.cn/tjsj/ndsj/

NDRC, National Development and Reform Commission of China, 2005. China Green Lights Development Report (2004). China Elect. Pow. Press, Beijing.

Nenes, A., Pandis, S. N., and Pilinis, C.: ISORROPIA: A new thermodynamic equilibrium model for multiphase multicomponent inorganic aerosols, Aquat. geochem., 4, 123-152, 1998.

Pan, Y.: Actual Effect Tracking and Analysis of a LED Road Lighting Upgrading Project, China Light & Lighting, 2018.

Román, M. O., and Stokes, E. C.: Holidays in lights: Tracking cultural patterns in demand for energy services, Earth. Future, 3, 182-205, 2015.

SCIO, State Council Information Office of China, 2006. NDRC press conference on Green Lights Program. Available from: http://www.scio.gov.cn/xwfbh/gbwxwfbh/xwfbh/fzggw/document/313370/313370.htm, last acceesed on Semptember 5, 2018

Seinfeld, J. H., Pandis, S. N., and Noone, K.: Atmospheric Chemistry and Physics: From Air Pollution to Climate Change, Environ. Sci. Policy Sust. Dev., 40, 26-26, 1998.

Tie, X., Brasseur, G., Emmons, L., Horowitz, L., and Kinnison, D.: Effects of aerosols on tropospheric oxidants: A global model study, J. Geophys. Res. Atmos., 106, 22931-22964, 2001.

Tie, X., Madronich, S., Walters, S., Zhang, R., Rasch, P., and Collins, W.: Effect of clouds on photolysis and oxidants in the troposphere, J. Geophys. Res., 108, 2003.

Tie, X., and Cao, J.: Aerosol pollution in China: Present and future impact on environment, Particuology, 8, 426-431, 2010.

Tie, X., Huang, R. J., Cao, J., Zhang, Q., Cheng, Y., Su, H., Chang, D., Pöschl, U., Hoffmann, T., and Dusek, U.: Severe Pollution in China Amplified by Atmospheric Moisture, Sci. Rep., 7, 15760, 2017.

Tong, D., Zhang, Q., Liu, F., Geng, G., Zheng, Y., Xue, T., Hong, C., Wu, R., Qin, Y., Zhao, H., Yang, L., He, K., 2018. Current Emissions and Future Mitigation Pathways of Coal-Fired Power Plants in China from 2010 to 2030. Environmental Science & Technology 52, 12905-12914.

Wang, S., and Hao, J.: Air quality management in China: Issues, challenges, and options, J. Environ. Sci., 24, 2-13, 2012.

Wang, Y., Zhang, Q., Jiang, J., Zhou, W., Wang, B., He, K., Duan, F., Zhang, Q., Philip, S., and Xie, Y.: Enhanced sulfate formation during China's severe winter haze episode in January 2013 missing from current models, J. Geophys. Res. Atmos., 119, 10,425-410,440, 2015a.

Wang, Y. J.: Study on energy saving technology of urban road lighting LED street lighting, Heilongjiang Science, 2017.

Wang, Z., Pan, L., Li, Y., Zhang, D., Ma, J., Sun, F., Xu, W., and Wang, X.: Assessment of air quality benefits from the national pollution control policy of thermal power plants in China: A numerical simulation, Atmos. Environ., 106, 288-304, 2015b.

Wesely, M.: Parameterization of surface resistances to gaseous dry deposition in regional-scale numerical models, Atmos. Environ., 23, 1293-1304, 1989.

Xie, Y., Yang, Y., and Polytechnic, F.: Discussion on the application of LED lighting power drive technology, Electron. Test, 2016.

Xue, J., Yuan, Z., Griffith, S. M., Yu, X., Lau, A. K. H., and Yu, J. Z.: Sulfate Formation Enhanced by a Cocktail of High NOx, SO2, Particulate Matter, and Droplet pH during Haze-Fog Events in Megacities in China: An Observation-Based Modeling Investigation, Environ. Sci. Technol., 50, 7325, 2016.

Yu, C., and Zhou, D.: Evaluation of the implementation of China's green lights program, Energy China, 2, 8-11, 2001.

Zhang, H., Li, J., Qi, Y., Jian, Z. Y., Wu, D., Yuan, C., He, K., and Jiang, J.: Source apportionment of PM 2.5 nitrate and sulfate in China using a source-oriented chemical transport model, Atmos. Environ., 62, 228-242, 2012.

Zhang, Q., Streets, D. G., Carmichael, G. R., He, K., Huo, H., Kannari, A., Klimont, Z., Park, I., Reddy, S., and Fu, J.: Asian emissions in 2006 for the NASA INTEX-B mission, Atmos. Chem. Phys., 9, 5131-5153, 2009.

Zhao, Y., Zhang, J., and Nielsen, C. P.: The effects of recent control policies on trends in emissions of anthropogenic atmospheric pollutants and CO2 in China, Atmos. Chem. Phys., 13, 487-508, 10.5194/acp-13-487-2013, 2013.

Zheng, B., Gao, F., and Guo, X.: Survey Analysis of Lighting Power Consumption in China, China Light & Lighting, 2016.

Tab.1

Table 1. Effective Luminous Efficacy (ELE) with and without the GLP

	Cluster[a]	Lamp type	LE[a]	P[b]	ELE
Low-efficiency lamps					ELE_{no-GLP}
Lower range	C1	HPM	50[a]	31.6%[b]	52.8
	C2	ILs	15[a]	19.7%[b]	
	C3	T12/T10	70	48.7%[b]	
Upper range	C1	HPM	50[a]	31.6%[b]	57.7
	C2	ILs	15[a]	19.7%[b]	
	C3	T12/T10	80[a]	48.7%[b]	
High-efficiency lamps					ELE_{GLP}
Lower range	C1, C2, C3	LED	150[c]	32.0%[c]	96.2
	C1	HPS/MH	70[a]	21.5%[d]	
	C2	CFLs	50[a]	13.4%[e]	
	C3	T8/T5	80[a]	33.1%[e]	
Upper range	C1, C2, C3	LED	150[c]	32.0%[c]	120.9
	C1	HPS/MH	140[a]	21.5%[d]	
	C2	CFLs	60[a]	13.4%[e]	
	C3	T8/T5	105[a]	33.1%[e]	

P: the proportion of lighting electricity consumed by specific cluster lamps to the total lighting electricity consumption

a. The values were taken from Guo et al. (2017).

b. The values were taken from Zheng et al. 2016

c. The values were evaluated based on Gao et al., 2016

d. The values were estimated based on Zheng et al., 2016 and Ding et al., 2017

e. The values were estimated based on Refs of a, b, c, and d.

LE and ELE: (lm/W)

LED: light-emitting diode

HPM lamps: High Pressure Mercury-vapor lamps

HPS lamps: High Pressure Sodium lamps MH lamps: Metal Halide

ILs: Incandescent lamps CFLs: Compact Fluorescent Lamps

T12/T10: T12/T10 fluorescent tubes T5/T8: T5/T8 fluorescent tubes

C1: outdoor lighting, such as road lights

C2: residential applications, such as households

C3: commercial and industrial buildings

Tab.2

Table 2. Coal consumptions, and emissions for the reference case (REF), the limit cases of low (SEN-GLP-low) and high (SEN-GLP-high)

Species	REF (100%)	SEN-GLP-low (+6.7%)	SEN-GLP-high (+18.0%)
Coal consumption for coal-fired power in China in 2015 (Tg)			
	1793.2	119.7	323.3
Emissions from power in 3 cases in the domain in Dec. 2015 (Gg)			
NOx	299.1	299.1+20.0	299.1+53.8
SO_2	103.7	103.7+6.9	103.7+18.7
$PM_{2.5}$	31.1	31.1+2.1	31.1+5.6
Others	X	106.7X%	118.0X%

Figure Captions

Figure 1. The spatial distributions of the Nighttime-light data (NLT) from DMSP/OLS DN values in (a) 1992 and in (b) 2013.

Figure 2. Coal-fired power electricity and associated coal consumption for power generation, and the emissions of NOx, SO_2, and $PM_{2.5}$ from thermal power plants from 2000 to 2015 in China.

Figure 3. The horizontal domain of the model (WRF-CHEM), with the location of sampling sites (shown by the green crosses), and topographical conditions of the NCP, which are surrounded by the Mountains of Yan and Tai in the north and west, respectively.

Figure 4. The **(a)** lower and **(b)** upper limits of potential coal-savings induced by the GLP.

Figure 5. The temporal variations of predicted (red lines) and observed (black dots) profiles of near-surface mass concentrations of $PM_{2.5}$, NO_2, SO_2, and CO averaged over all ambient monitoring sites in the NCP during December 2015.

Figure 6. The spatial comparisons of predicted and observed episode-average mass concentrations of $PM_{2.5}$, NO_2, and SO_2. **(a)** Statistical comparison of predicted and observed mass concentrations, with the correlation coefficient (*r*). Horizontal distributions of predictions (color contour) and observations (colored circles) of **(b)** $PM_{2.5}$, **(c)** NO_2, and **(d)** SO_2, along with the simulated wind fields (black arrows).

Figure 7. The potential emission reductions for low (left panels) and high (right panels) limit cases induced by the GLP, including the mass rates change of **(a)** NO_x, and **(b)** SO_2. The total emission reductions are also shown in the rectangle.

Figure 8. The lower (left panels) and upper (right panels) episode-averaged variations induced by GLP, including the mass concentrations (μg m^{-3}) of **(a)** $PM_{2.5}$, **(b)** NO_2, and **(c)** SO_2. The results refer to the spatial variations between the REF case and the SEN-GLPs case (REF − SNE-GLPs).

Fig. 1

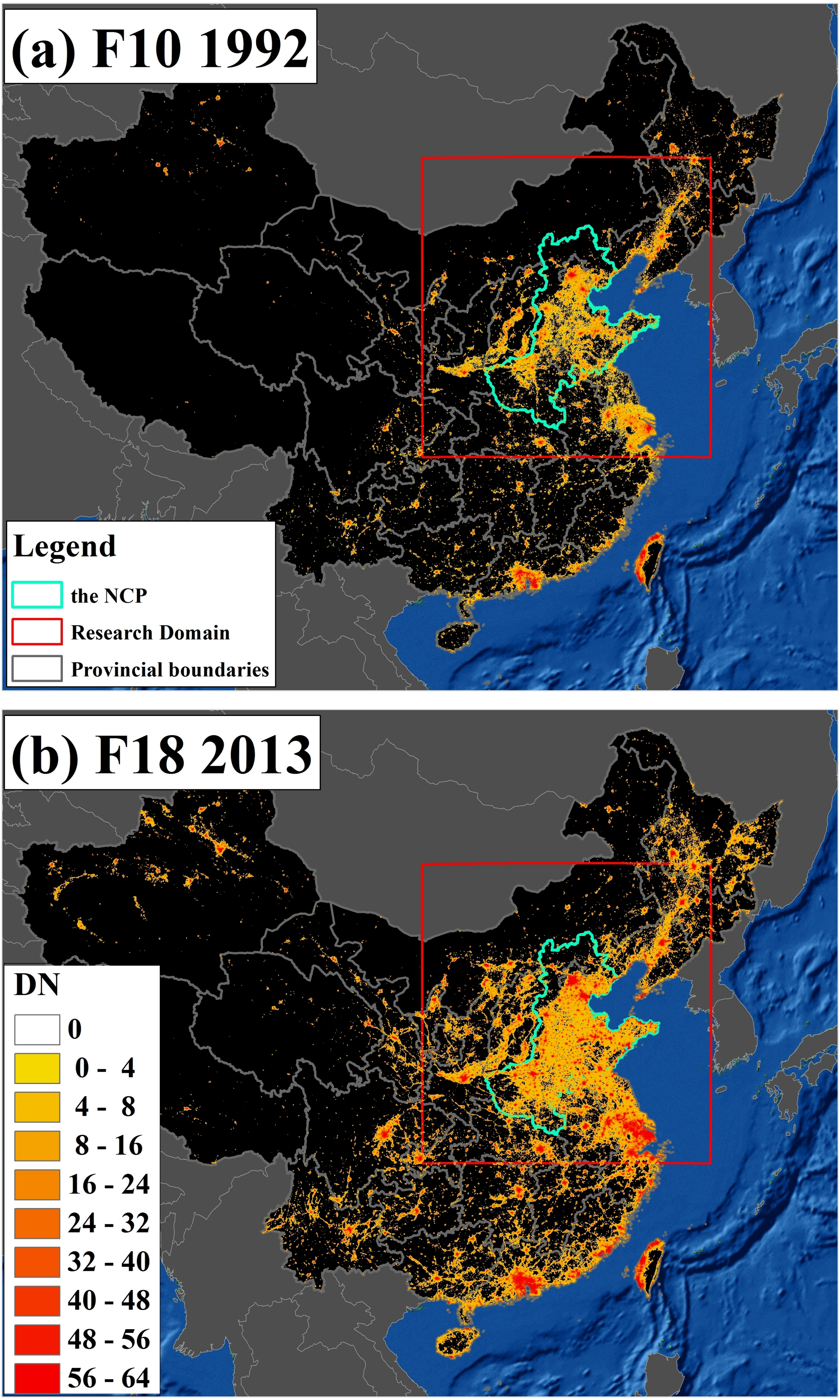

Figure 1. The spatial distributions of the Nighttime-light data (NLT) from DMSP/OLS DN values in (a) 1992 and in (b) 2013.

Fig. 2

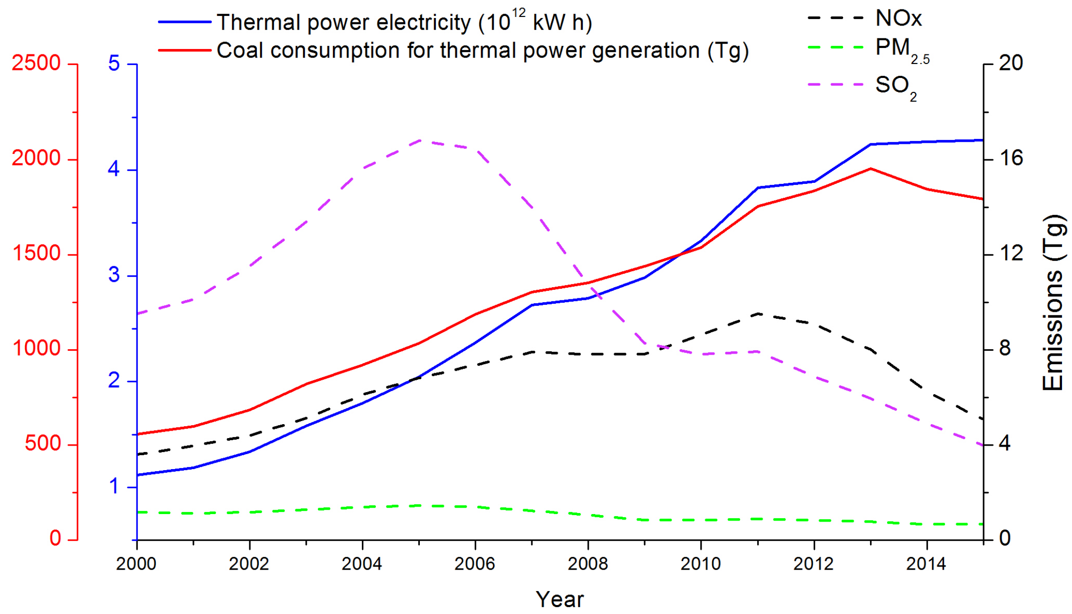

Figure 2. The thermal power electricity, the coal consumption for thermal power generation, and the emissions of NOx, SO_2, and $PM_{2.5}$ from thermal power plants from 2000 to 2015 in China.

Fig. 3

Figure 3. The horizontal domain of the model (WRF-CHEM), with the location of sampling sites (shown by the green crosses), and topographical conditions of the NCP, which are surrounded by the Mountains of Yan and Tai in the north and west, respectively.

Fig. 4

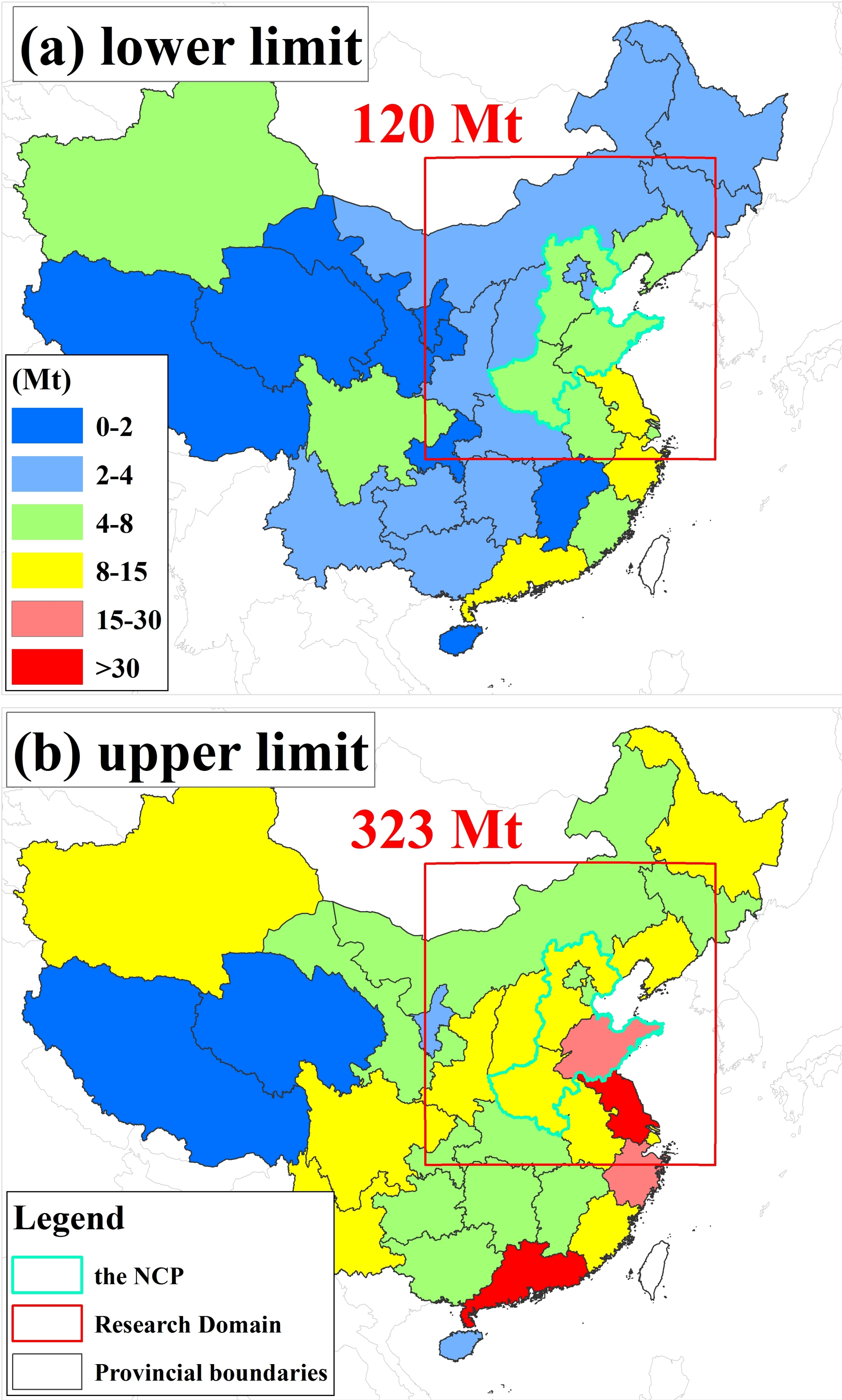

Figure 4. The **(a)** lower and **(b)** upper limits of potential coal-savings induced by the GLP.

Fig. 5

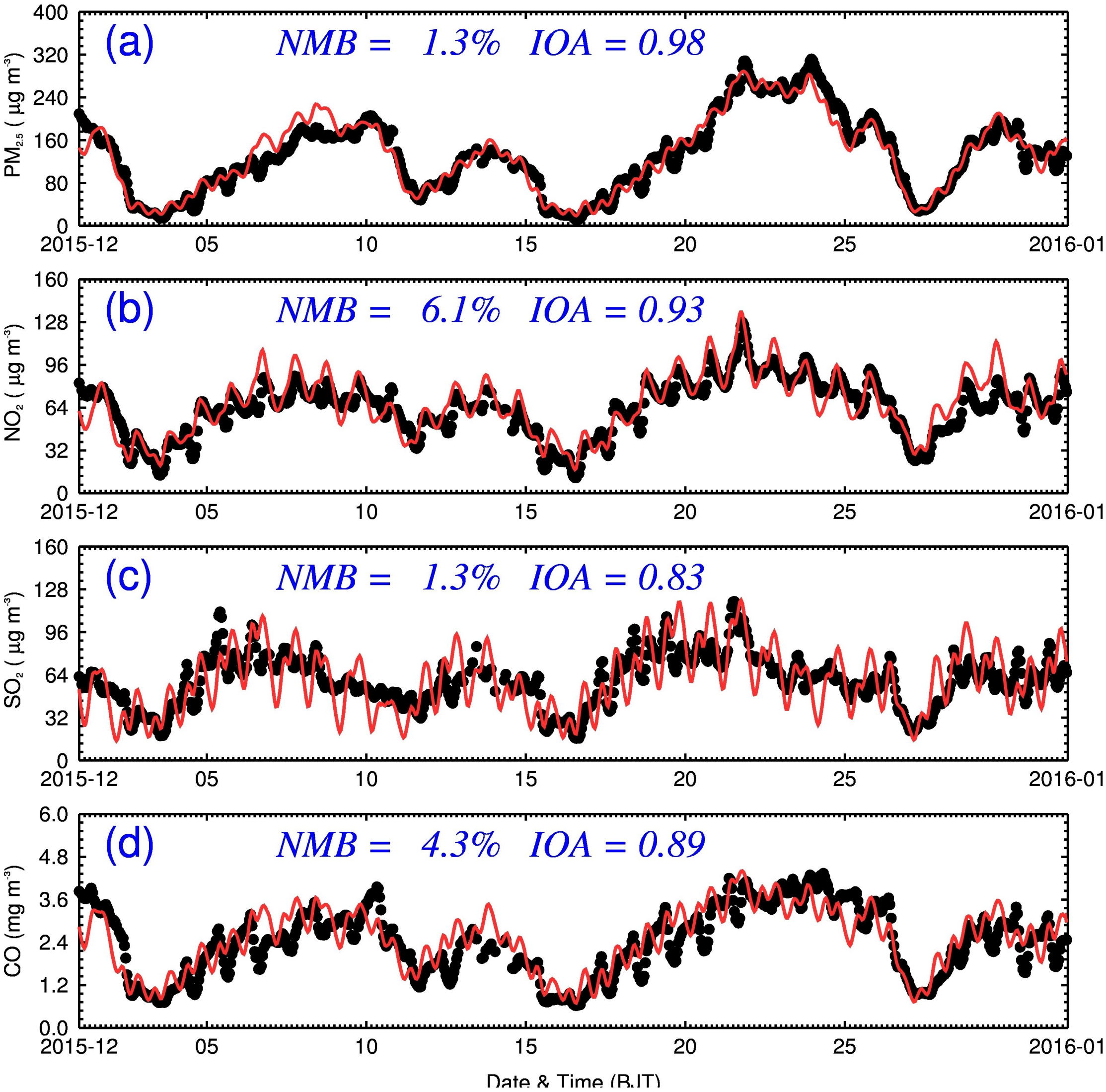

Figure 5. The temporal variations of predicted (red lines) and observed (black dots) profiles of near-surface mass concentrations of $PM_{2.5}$, NO_2, SO_2, and CO averaged over all ambient monitoring sites in the NCP during December 2015.

Fig. 6

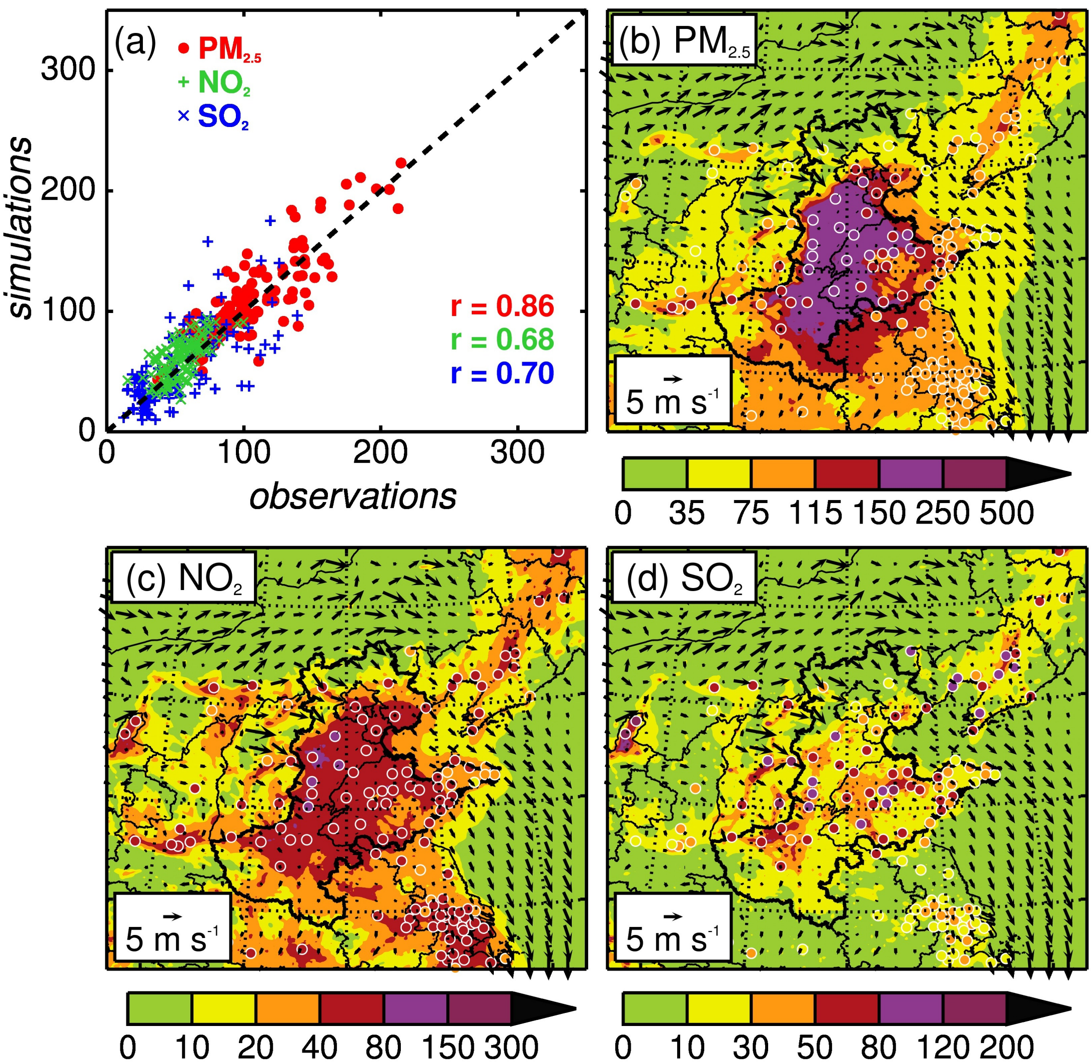

Figure 6. The spatial comparisons of predicted and observed episode-average mass concentrations of $PM_{2.5}$, NO_2, and SO_2. **(a)** Statistical comparison of predicted and observed mass concentrations, with the correlation coefficient (*r*). Horizontal distributions of predictions (color contour) and observations (colored circles) of **(b)** $PM_{2.5}$, **(c)** NO_2, and **(d)** SO_2, along with the simulated wind fields (black arrows).

744 **Fig. 7**

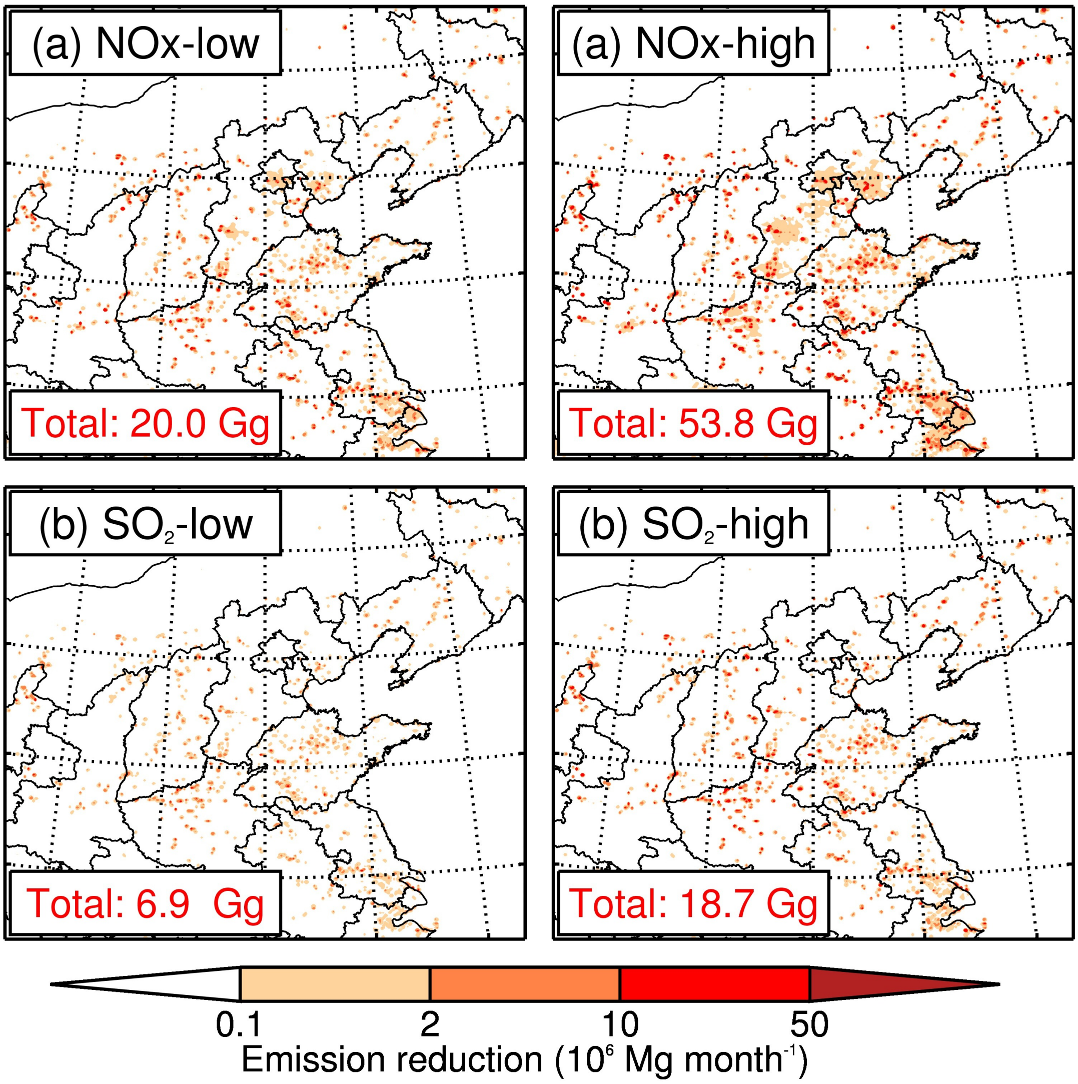

745

746 **Figure 7.** The potential emission reductions for low (left panels) and high (right panels) limit

747 cases induced by the GLP, including the mass rates change of **(a)** NO_x, and **(b)** SO_2. The total

748 emission reductions are also shown in the rectangle.

Fig. 8

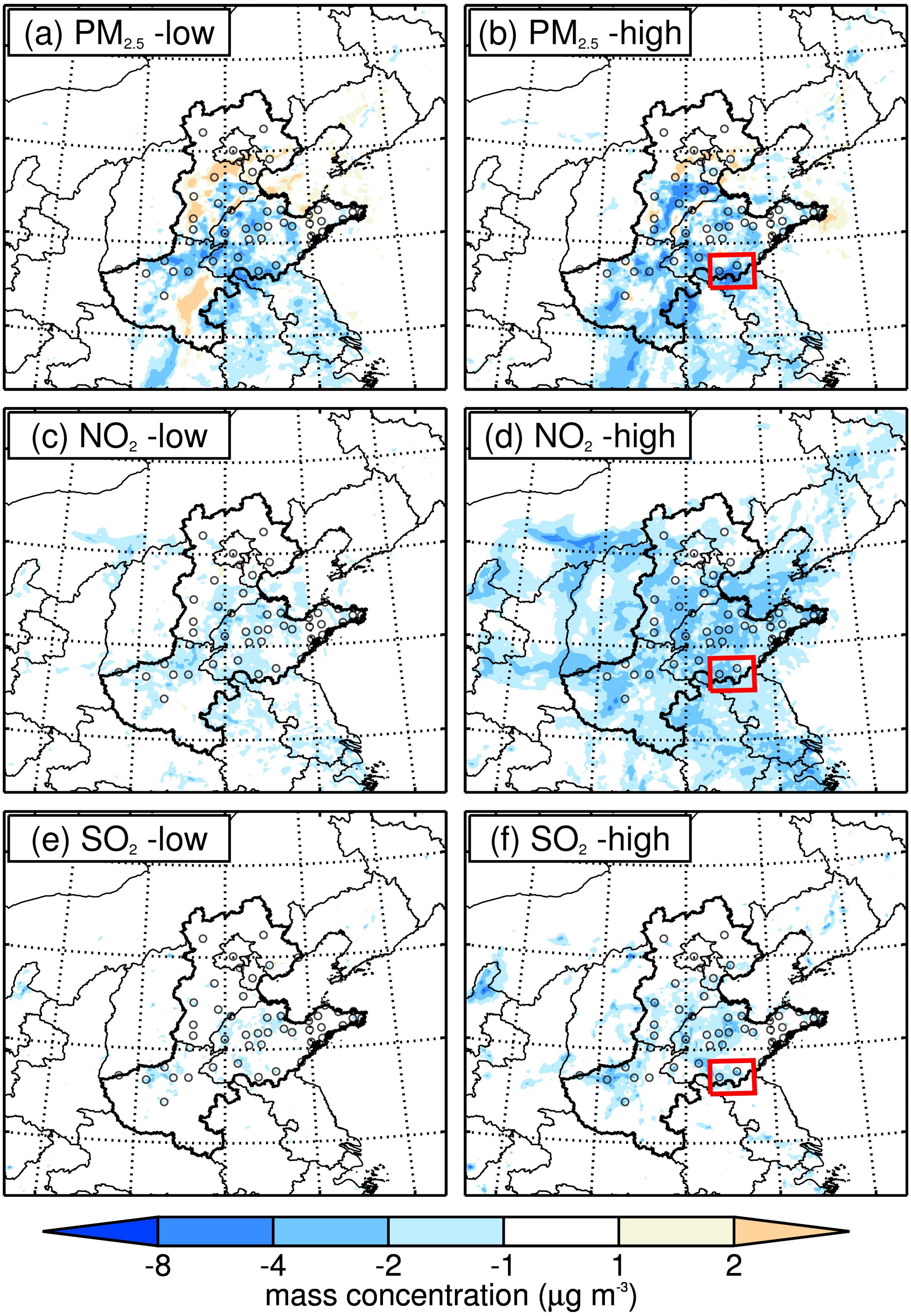

Figure 8. The lower (left panels) and upper (right panels) episode-averaged variations induced by GLP, including the mass concentrations (μg m^{-3}) of **(a)** $PM_{2.5}$, **(b)** NO_2, and **(c)** SO_2. The results refer to the spatial variations between the REF case and the SEN-GLPs case (REF − SNE-GLPs). The red-squares display the areas with high $PM_{2.5}$ changes induced by the GLP.